

RSC Advances



This is an *Accepted Manuscript*, which has been through the Royal Society of Chemistry peer review process and has been accepted for publication.

Accepted Manuscripts are published online shortly after acceptance, before technical editing, formatting and proof reading. Using this free service, authors can make their results available to the community, in citable form, before we publish the edited article. This *Accepted Manuscript* will be replaced by the edited, formatted and paginated article as soon as this is available.

You can find more information about *Accepted Manuscripts* in the [Information for Authors](#).

Please note that technical editing may introduce minor changes to the text and/or graphics, which may alter content. The journal's standard [Terms & Conditions](#) and the [Ethical guidelines](#) still apply. In no event shall the Royal Society of Chemistry be held responsible for any errors or omissions in this *Accepted Manuscript* or any consequences arising from the use of any information it contains.



New Approach for the Reduction of Graphene Oxide with Triphenylphosphine Dihalide

Received 00th January 20xx,
Accepted 00th January 20xx

Hong-Suk Shin,^{acd} Ki Woong Kim,^{bd} Yong-goo Kang,^c Sung Myung,^b Jong Seung Kim,^c Ki-Seok An,^b Ill Young Lee^{*a} and Sun Sook Lee^{*b}

DOI: 10.1039/x0xx00000x

www.rsc.org/

We developed a one-flask method for the thermal reduction of graphene oxide (GO) with triphenylphosphine dihalide (Ph₃PX₂) at 180°C. Our approach offers a potential to cost-effective mass-production of graphene nanosheets under mild and environmentally friendly conditions and to avoid the use of strong acids or reducing agents. Significantly, this reduced graphene oxide (rGO) by utilizing Ph₃PX₂ reductant has a C/O ratio higher than 15 and an electrical conductivity of 400 S/cm, which indicate that this synthetic method allows us to achieve graphene nanosheets with high quality when comparing with previous reduction methods.

Graphene, which consists of a single layer of sp² hybridized carbon atoms with a regular hexagonal pattern,¹ has been of interest in both the experimental and theoretical scientific communities due to its extraordinary electrical, optical, mechanical, and thermal properties.²⁻⁶ These properties offer the potential for many practical applications including nanoelectronics,⁷⁻⁹ chemical/biosensors,¹⁰⁻¹³ ultracapacitors,¹⁴⁻¹⁶ and composite reinforcement.¹⁷ However, these application require not only the synthesis of high-quality graphene, but also huge quantities of graphene in the form of nanosheets. Recently, several approaches such as chemical vapor deposition (CVD), epitaxial growth,¹⁸⁻²¹ mechanical exfoliation,²² and chemical reduction have been developed to fabricate and develop electrical devices based on graphene layers. Among these methods, the chemical reduction of graphene oxide (GO) is one of the promising routes for the large scale synthesis of graphene for commercial applications.²³ Here, GO with reactive oxygen functional

groups including epoxy, hydroxyl, carbonyl, ester and carboxylic acid groups is generally reduced by a strong acid during the reduction process. For example, many research groups have used reducing agents such as hydrazine,²⁴ N,N-dimethylacetamide,²⁵ hydroquinone,²⁶ NaBH₄,²⁷ or LiAlH₄²⁹ in order to reduce oxygen-containing groups and restore sp³ bonds of GO to sp² bonds. Although strong reducing agents such as LiAlH₄ are effective for the graphene reduction, LiAlH₄ agent is not available for general use in commercial applications because of the potential hazards of this agent. Also, harmless reducing agents are not effective for the reduction of hydroxyl groups on GO surfaces toward sp² hybridized graphene. In previous studies,³⁰⁻³¹ Strong acid HX (X=I or Br) and MI₂ (M=Mg, Zn or Fe) have been also utilized as reduction reagents. Here, the hydroxyl group was substituted with a halide anion followed by dehalogenation or dehydrohalogenation.³² However, this method has the limitation for their applications to mass production of graphene sheets, because HX or acidic solvent is highly corrosive. Although biocompatible reductants such as vitamin C,³³⁻³⁴ melatonin,³⁵ glucose/Fe,³⁶ polyphenols of green tea,³⁷ ginseng,³⁸ protein bovine serum albumin (BSA),³⁹ NADH,⁴⁰ and even bacteria⁴¹ have been used in reducing process, these methods with these biocompatible agents are not effective for the mass production of high quality graphene sheets. For instance HBr/water⁴² resulted in the insufficient reduction for rGO with aryl alcohol and aryl carboxylic acid. Importantly, the optimized reaction time for rGO with HI/TFA (C/O-ratio 12)⁴³ or HI/AcOH (C/O-ratio 6)⁴⁴ was about 40 hours, which condition is need to shorten the reaction time for the mass graphene production. Zhao *et al.*⁴⁵⁻⁴⁶ also reported that a synthesis approach for the graphene nanosheets by etching of the graphite using plasma treatments. This method with plasma technique still has limitations that large-scale plasma device is still required for the mass-fabrication of nanosheets. In recent study,⁴⁷ triphenylphosphine (PPh₃) was used for modifying the graphene quantum dots structure (GQDs). Here, the introduction of PPh₃ to GQDs to get chemical C-PPh₃ bond for pectral modulation and high quantum yield was carried out

^a Eco-Friendly New Materials Research Center, Korea Research Institute of Chemical Technology, 141, Gajeong-ro, Yuseong-gu, Daejeon, Republic of Korea, 34114. E-mail: iylee@kRICT.re.kr

^b Thin Film Materials Research Center Korea Research Institute of Chemical Technology, 141, Gajeong-ro, Yuseong-gu, Daejeon, Republic of Korea, 34114. E-mail: sunsook@kRICT.re.kr

^c Department of Chemistry, Korea University, 145, Anam-ro, Seongbuk-gu, Seoul, Republic of Korea, 02841.

^d These authors contributed equally to this work

† Electronic Supplementary Information (ESI) available: general reduction process and details of the setup. See DOI: 10.1039/x0xx00000x

in autoclave at 72 °C for 72h. In addition, triphenylphosphine dibromide (Ph_3PBr_2) and triphenylphosphine diiodide (Ph_3PI_2), known as Appel agents,⁴⁸ have been utilized to convert chemically an acid to an acid halide,⁴⁹ an epoxide to a *vic*-dihalide,⁵⁰ or an alcohol such as phenol to a halide.⁵¹ However, when Appel reagents were applied for the reduction condition of GO, the proper heating condition was required because of the strong binding between a halogen and carbon of graphene.

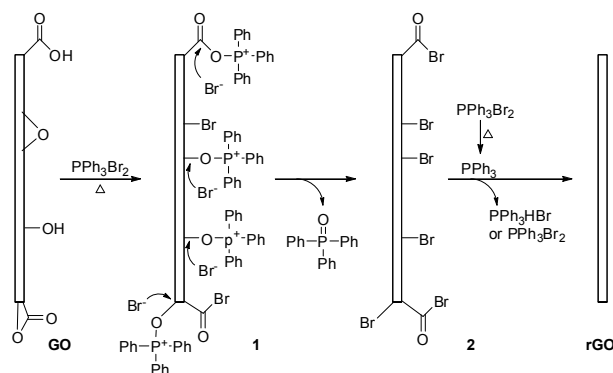


Fig. 1 Schematic representation showing the reducing chemistry of GO conversion to rGO.

In the present study, triphenylphosphine dihalide (Ph_3PX_2) was used to reduce GO nanosheets by heating GO with Ph_3PBr_2 at 180 °C for 1h. First, GO was prepared from natural graphite according to the modified Hummers method.⁵²⁻⁵³ Natural graphite flakes were oxidized into graphite oxide using NaNO_3 , H_2SO_4 , KMnO_4 , and H_2O_2 . The as-obtained graphite oxide was washed several times by using centrifugation. The product was then dispersed in distilled water and the exfoliated GO sheets were subjected to ultra-sonication. The crude graphite oxide was washed several times with 10% HCl solution during the centrifugation. The product was then washed with deionized water until the pH level was 4 and the exfoliated GO sheets were dried in vacuum oven at 40 °C for 12h. Although commercially available Ph_3PBr_2 (6mmol) could be used for the reduction of GO, PPh_3 was first dissolved in nitrogen-degassed acetonitrile (8ml), and bromine (6mmol) was added dropwise into the reaction mixture for 10 min at 0 °C for getting fresh Ph_3PBr_2 . GO (100 mg) suspended in nitrogen-degassed acetonitrile was added to the Ph_3PBr_2 in acetonitrile solution, and acetonitrile and bromine species in reaction mixture slowly distilled out at 90 °C under atmospheric pressure. The resulting concentrated residue was heated at 180 °C for 1 h under a nitrogen atmosphere. After cooling down to room temperature, the resulting solid was dissolved in chloroform and stirred for 30 min. The rGO dispersion was filtered through PTFE membranes and filter paper and then washed successively with methanol, ethanol, and dichloromethane. Finally, the reduced product was dried overnight in a vacuum oven at 40 °C, and rGO nanosheets were collected as a black filter cake for further use.

Our proposed mechanism to reduce GO to rGO is illustrated in Fig. 1. Generally, the conversion of acid,⁴⁹ cyclic ester,⁵⁴ epoxide⁵⁰ and aryl alcohol^{51,55} functional group into each

bromine substituent has been extensively studied and mechanism carefully proposed. The reaction of acid, cyclic ester, aryl alcohol and epoxide group on GO with Ph_3PBr_2 may give ionic phosphonium intermediate **1** followed by substitution by bromide ion to proceed by forming anticipated brominated rGO intermediate **2** with the generation of triphenylphosphine oxide. After that, rGO can be formed by reductive debromination by generating triphenylphosphine from Ph_3PBr_2 by thermal heating and further aromatization of **2** which mechanism would be similar to debromination at activated positions such as fullerene or α -bromoketone by triphenylphosphine as mechanism proposed in the literatures.⁵⁶⁻⁵⁹ In this reduction procedures, we could isolate and purify triphenylphosphine oxide (mp = 150 - 157 °C) as a side product of Appel conditions⁴⁸ from the washing organic solvents of rGO. Significantly, since this synthetic method is a cost effective and scalable procedure, to apply this nanosheet to various photonic devices such as solar cells, light-emitting diodes photodetectors is currently under investigation.

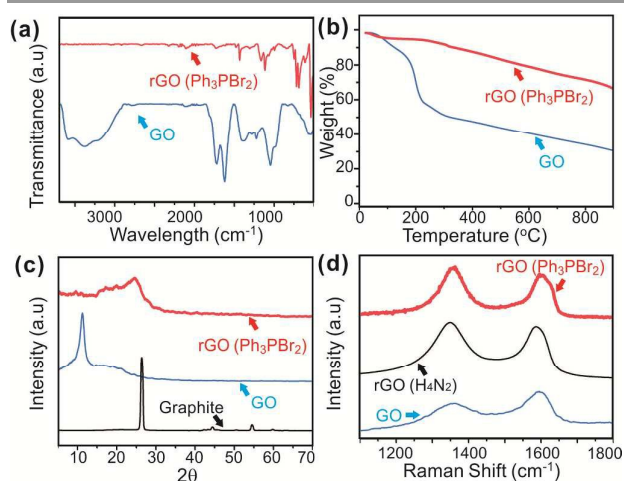


Fig. 2 (a) FTIR transmittance of GO and rGO (Ph_3PBr_2). (b) TGA curves of GO and rGO (Ph_3PBr_2) in an N_2 atmosphere. (c) XRD patterns of graphite, GO, and rGO (Ph_3PBr_2). (d) Raman spectra of GO, rGO (H_2N_2), and rGO (Ph_3PBr_2).

Fourier transform infrared spectroscopy (FTIR) was used to determine the functional groups on GO and rGO (Fig. 2a).^{26,28,33,36} In the FTIR spectrum of GO, strong bands due to C=O and C–O stretching vibrations in COOH groups were present at 1727 and 1045 cm^{-1} , respectively. The strong band at 1620 cm^{-1} was assigned to the vibration of adsorbed water molecules and skeletal vibrations of the graphene sheets. The broad band at 3358 cm^{-1} , which is particularly visible in unfunctionalized GO, corresponded to O–H stretching vibrations of carboxylic groups and adsorbed water molecules.^{35,39,60-63} bands at 1223 cm^{-1} and 1040 cm^{-1} corresponded to the epoxy CO and alkoxy CO stretching vibrations, respectively. In the rGO spectrum, the bands at 3358 cm^{-1} (OH), 1223 cm^{-1} (epoxy), and 1040 cm^{-1} (alkoxy) became dramatically small. Only small peaks at 1727 cm^{-1} and 1045 cm^{-1} due to C=O and C–O were observed after the reduction.

We also used thermogravimetric analysis (TGA) to confirm the thermal stability of GO and rGO reduced with Ph_3PBr_2 (Fig. 2b). Here, GO and rGO were heated in a nitrogen atmosphere from room temperature to 900 °C at a rate of 10 °C/min. The weight of the GO decreased at temperatures higher than 100 °C due to loss of water molecules on the hydrophilic GO surface. A large mass loss occurred at about 200 °C, possibly due to decomposition of labile, oxygen-containing functional groups. rGO had a much greater thermal stability than did GO, indicating that GO functional groups containing oxygen were removed successfully during reduction with Ph_3PBr_2 .

In the X-ray diffraction (XRD) analysis of graphite, GO, and rGO, shown in Fig. 2c, graphite demonstrated a major diffraction peak at $2\theta \approx 26.3^\circ$. GO had a diffraction peak at $2\theta \approx 10.3^\circ$, which corresponds to an interlayer d-spacing of 0.84 nm. After the reduction process, the peak at $2\theta \approx 10.3^\circ$ was no longer present in the GO XRD pattern, and rGO had a broad peak at $2\theta \approx 24^\circ$, which was attributed to the agglomeration of graphene sheets.²⁷ Hydrazine (N_2H_4) is a common and effective reducing agent for converting from GO to rGO via hydrothermal treatment. However, hydrazine is highly toxic, explosive chemical and can potentially functionalize the GO with nitrogen heteroatoms. We used Raman spectroscopy to compare the structural properties of GO, rGO reduced by hydrazine, and rGO reduced by Ph_3PBr_2 . Raman spectra were measured at an excitation of 514 nm, and all spectra were normalized to the G-band. Fig. 2d shows the Raman spectrum of GO, in which the Raman fingerprints of GO, including the D-band (1358 cm^{-1}) and G-band (1596 cm^{-1}), are apparent. The Raman spectrum of rGO reduced by hydrazine had a D-band at 1349 cm^{-1} and a G-band at 1589 cm^{-1} , and rGO reduced by Ph_3PBr_2 had a D-band at 1357 cm^{-1} and a G-band at 1590 cm^{-1} . The G-band of rGO reduced by Ph_3PBr_2 exhibited a significant redshift, similar to that of rGO reduced by hydrazine. In addition, the I_D/I_G ratio increased from 0.8 (GO) to 1.0 (rGO by Ph_3PBr_2), indicating that the graphene domain decreased during the reduction process. This result indicates that our reducing method using Ph_3PBr_2 is a good candidate for the reduction method that does not require strong acidic conditions or highly toxic agents such as hydrazine. Additionally, we took AFM topography images of a GO to measure the stability during reducing process (Figure S3 in Supportin Information). The results indicate that we achieved GO nanosheets with $\sim 1.1\text{ nm}$. It is clear that we can obtain uniform rGO flakes without the structure destruction of GO nanosheets after reduction processes.

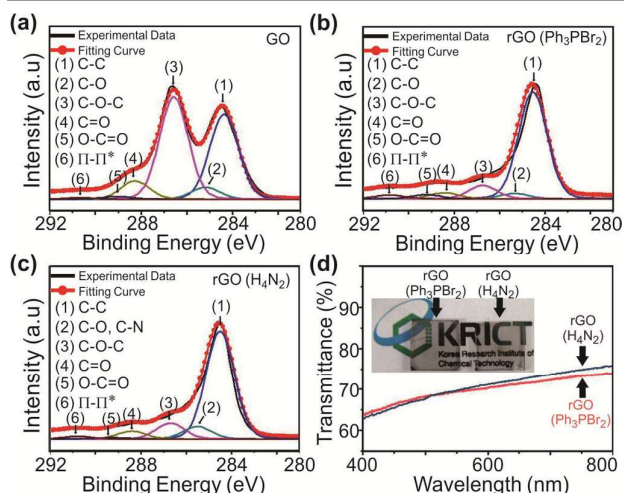


Fig. 3 The C1s peak in the XPS spectra of (a) GO, (b) rGO (Ph_3PBr_2), and (c) rGO reduced by hydrazine. (d) Optical transmittance of rGO reduced by Ph_3PBr_2 and rGO thin film on glass reduced by hydrazine vapor.

X-ray photoelectron spectroscopy (XPS) was used to quantify the atomic compositions and stoichiometric ratios of GO, rGO reduced by hydrazine, and rGO by Ph_3PBr_2 . Fig. 3(a)-(c) show the core level of C 1s XPS spectra of GO, rGO reduced by Ph_3PBr_2 , and rGO reduced by hydrazine. As shown in Fig. 3(a), XPS spectra of GO exhibits six peaks at 284.5, 285.3, 286.7, 288.4 and 289.2, which were assigned to C-C, C-O, C-O-C, C=O and O-C=O functional groups, respectively. In cases of rGO reduced by Ph_3PBr_2 and rGO by hydrazine, the intensity of the oxygenated groups in the C1s peak was reduced dramatically, compared to GO. This result shows that the oxygen-containing group was eliminated during the reduction process, and the sp^2 carbon peaks were recovered. Also, a new carbon peak at 290.8 eV corresponding to $\pi-\pi^*$ satellite was appeared at a high binding energy, which corresponds to a carbon bound to another atom. Significantly, the C/O ratio of rGO reduced by hydrazine is only 7.9, while that of rGO by Ph_3PBr_2 is 16. Also, rGO by Ph_3PBr_2 has a larger C/O ratio than rGO by dehydrobromination in a previous work.⁴¹

Fig. 3(d) shows the optical transmittances at 550 nm of thin films based on rGO reduced by hydrazine and rGO reduced by Ph_3PBr_2 . Thin GO film on a transparent substrate was prepared by spin-coating, and the sheet resistance was measured by using the four-point probe technique. The sheet resistance of rGO reduced by hydrazine was $350.6\text{ k}\Omega/\text{sq}$ at 69.4%, and the film based on rGO reduced by Ph_3PBr_2 had a sheet resistance of $26.8\text{ k}\Omega/\text{sq}$ with an optical transmittance of 69.7%.

The relative atomic ratio of functional groups of GO, rGO reduced by Ph_3PBr_2 , and rGO reduced by hydrazine were determined by XPS analysis and are summarized in Table 1. rGO reduced by Ph_3PBr_2 had a higher percentage of C-C (sp^2) after the reduction process and a hetero carbon percentage of 18.8%. The hetero carbon percentage of rGO reduced by Ph_3PBr_2 was lower than that of rGO reduced by hydrazine. This result indicates that our approach may allow us to mass-produce rGO nanosheets with high quality. The atomic percentages of rGO reduced by Ph_3PX_2 in various synthetic

conditions according to XPS analysis are also given in Table 2. GO was reacted with Ph_3PBr_2 (6 equiv) at 180 °C without solvent to yield rGO containing 5.8% oxygen. In a similar reaction using PPh_3I_2 instead of Ph_3PBr_2 , rGO contained 6.1% oxygen. When we increased the GO weight up to gram scale in this condition, the rGO was prepared up to gram scale with similarly C/O ratio. In addition, the dependence of the reduction reaction on temperature was investigated. When the reaction was conducted with Ph_3PBr_2 (6mmol) under neat conditions or in chlorobenzene at 120 °C, the rGO contained 11.2% or 10.5% oxygen, respectively. rGO and Ph_3PBr_2 (6mmol) in DMF by microwave assist reaction at 120 °C (400W) had a lower oxygen percent (7.1%) than with an ultrasonic-assisted reaction in acetonitrile at 40 °C (O : 8.6%). Refluxing GO and Ph_3PBr_2 (6mmol) in acetonitrile provided bromine attached partially reduced GO (C: 84.8, O: 13.0 and Br: 1.4% content) as expected in proposed mechanism (Fig. 1). When only PPh_3 without dihalide was used, the rGO contained 18.3% oxygen, which was lower than the 23.8% for rGO heated without reagents or solvent. The various phosphine reagents, solvents, and temperature were optimized to reduce GO as described in detail (37 reaction conditions) in the supporting information.

Table 1. Relative atomic ratios of functional groups determined by XPS analysis of GO, rGO reduced by Ph_3PBr_2 , and rGO reduced by hydrazine.

Sample	Relative Atomic Percentage (%)						Hetero-carbon (%)
	C-C	C-O, C-N	C-O-C	C=O	C=O-O	$\pi-\pi^*$	
GO	38.5	5.3	46.2	8.1	1.2	0.7	60.9
rGO (Ph_3PBr_2)	77.7	10.2	5.8	1.8	1.0	3.5	18.8
rGO (H_2N_2)	73.3	8.3	10.6	5.2	0.8	1.8	25.0

Table 2. XPS-determined atomic percentage of GO treated with Ph_3PX_2 for 1 hour in various reduction conditions.

Reagent (equiv)	Temp.(°C)	C (%)	O (%)
$\text{PPh}_3\text{Br}_2(6)/\text{neat}^*$	180	93.8	5.8
$\text{PPh}_3\text{I}_2(6)/\text{neat}^*$	180	93.1	6.1
$\text{PPh}_3\text{Br}_2(6)/\text{neat}^*$	120	88.4	11.2 ^a
$\text{PPh}_3\text{Br}_2(6)/\text{ClPh}$	120	88.1	10.5 ^a
$\text{PPh}_3\text{Br}_2(6)/\text{DMF}/\text{microwave}$	120	92.4	7.1
$\text{PPh}_3\text{Br}_2(6)/\text{CH}_3\text{CN}/\text{sonic wave}$	40	90.9	8.6
$\text{PPh}_3\text{Br}_2(6)/\text{CH}_3\text{CN}$	90	84.8	13.0 ^b
$\text{PPh}_3(6)/\text{neat}^*$	180	81.5	18.3
Pristine GO	-	64.2	35.4

* GO(100mg) and reagents(6mmol) were dispersed in CH_3CN and then reaction mixture was concentrated for neat reaction. ^a Br content: < 0.5%, ^b Br content: 1.4%

Conclusions

To summarize, we presented an efficient, operationally simple, mass production protocol to reduce GO by heating at 180°C with Ph_3PX_2 in a *one-flask process*. After the reaction mixture washed organic solvents and dried, rGO was C/O ratio higher than 15 and an electrical conductivity of 400 S/cm. Compared with previous methods using hydrazine or metal hydrides, Ph_3PX_2 is more commercially available, easier to handle, and more environmentally friendly, which makes this protocol attractive and highly practical for the graphene synthesis. Our easy synthesis method may provide new opportunities to mass-produce two-dimensional carbon materials in an environmental friendly manner.

Acknowledgements

This research was supported by a grant (2011-0031636) from the Center for Advanced Soft Electronics under the Global Frontier Research Program of the Ministry of Science, ICT and Future Planning, Korea and by a grant from the Technology Development Program for Strategic Core Materials funded by the Ministry of Trade, Industry & Energy, Republic of Korea (Project No. 10047758).

References

- 1 T. Szabo, O. Berkesi, P. Forgo, K. Josepovits, Y. Sanakis, D. Petridis and I. Dekany, *Chem. Mater.*, 2006, **18**, 2740-2749.
- 2 K. S. Novoselov, A. K. Geim, S. V. Morozov, D. Jiang, Y. Zhang and S. V. Dubono, *Science*, 2004, **306**, 666-669.
- 3 A. A. Balandin, S. Ghosh, W. Bao, I. Calizo, D. Teweldebrhan, F. Miao and C. Lau, *Nano Lett.*, 2008, **8**, 902-907.
- 4 M. J. Allen, V. C. Tung and R. B. Kaner, *Chem. Rev.* 2010, **110**, 132-145.
- 5 R. R. Nair, P. Blake, J. R. Blake, R. Zan, S. Anissimova, U. Bangert, A. P. Golovanov, S. V. Morozov, A. K. Geim, K. S. Novoselov and T. Latychevskaia, *Appl. Phys. Lett.*, 2010, **97**, 153102.
- 6 C. Lee, X. D. Wei, J. W. Kysar and J. Hone, *Science*, 2008, **321**, 385-388.
- 7 Ph. Avouris, *Nano Lett.*, 2010, **10**, 4285-4294.
- 8 S. Frank, *Nat. Nanotechnol.*, 2010, **5**, 487-496.
- 9 W. S. Lim, Y. Y. Kim, H. Kim, S. Jang, N. Kwon, B. J. Park, J. Ahn, I. Chung, B. H. Hong and G. Y. Yeom, *Carbon* 2012, **50**, 429-435.
- 10 F. Schedin, A. K. Geim, S. V. Morozov, E. W. Hill, P. Blake, M. I. Katsnelson and K. S. Novoselov, *Nat. Mater.*, 2007, **6**, 652-655.
- 11 G. Lu, L. Ocola and J. Chen *Appl. Phys. Lett.*, 2009, **94**, 083111.
- 12 O. Akhavan, E. Ghaderi and R. Rahighi, *ACS Nano*, 2012, **6**, 2904-2916.
- 13 L. Guo, H. B. Jiang, R. Q. Shao, Y. L. Zhang, S. Y. Xie, J. N. Wang, X. Li, F. Jiang, Q. Chen, T. Zhang and H. Sun, *Carbon*, 2012, **50**, 1667-1673.
- 14 X. Zhao, H. Tian, M. Zhu, K. Tian, J. J. Wang, F. Kang and R. A. Outlaw, *J. Power Sources*, 2009, **194**, 1208-1212.
- 15 J. Bae, M. K. Song, Y. J. Park, J. M. Kim, M. Liu and Z. L. Wang, *Angew. Chem. Int. Ed.*, 2011, **50**, 1683-1687.
- 16 Z. Li, J. Wang, X. Liu, S. Liu, J. Ou and S. Yang, *J. Mater. Chem.*, 2011, **21**, 3397-3403.
- 17 Y. Ni, L. Chen, K. Teng, J. Shi, X. Qian, Z. Xu, X. Tian, C. Hu, and Meijun Ma, *ACS Appl. Mater. Interfaces*, 2015, **7**, 11583-11591.

- 18 S. Y. Park, J. Park, S. H. Sim, M. G. Sung, K. S. Kim, B. H. Hong and S. Hong, *Adv. Mater.*, 2011, **23**, H263–267.
- 19 N. Li, X. Zhang, Q. Song, R. Su, Q. Zhang, T. Kong, L. Liu, G. Jin, M. Tang and G. Cheng, *Biomaterials*, 2011, **32**, 9374–9382.
- 20 C. Heo, J. Yoo, S. Lee, A. Jo, S. Jung, H. Yoo, Y. Lee and M. Suh, *Biomaterials*, 2011, **32**, 19–27.
- 21 N. Li, Q. Zhang, S. Gao, Q. Song, R. Huang, L. Wang, L. Liu, J. Dai, M. Tang and G. Cheng, *Sci. Rep.*, 2013, **3**, 1604.
- 22 G. Vignaud, M. S. Chebil, J. K. Bal, N. Delorme, T. Beuvier, Y. Grohens and A. Gilbaud, *Langmuir*, 2014, **30**, 11599–11608.
- 23 K. C. Chun and M. Pumera, *Chem. Soc. Rev.*, 2014, **43**, 291–312.
- 24 S. Park, J. An, J. R. Potts, A. Velamakanni, S. Murali and R. Ruoff, *Carbon*, 2011, **11**, 3019–3023.
- 25 W. Chen and L. Yan, *Nanoscale* 2010, **2**, 559–563.
- 26 C. Li, L. Li, L. Sun, Z. Pei, J. Xie and S. Zhang, *Carbon*, 2015, **89**, 74–81.
- 27 C. K. Chua and M. Pumera, *J. Mater. Chem. A.*, 2013, **1**, 1892–1898.
- 28 Z. Yang, Q. Zheng, H. Qiu, J. Li and J. Yang, *New Carbon Materials*, 2015, **30**, 41–47.
- 29 A. Ambrosi, C. K. Chua, A. Bonanni and M. Pumera, *Chem. Mater.*, 2012, **24**, 2292–2298.
- 30 S. Pei, J. Zhao, J. Du, W. Ren and H. M. Cheng, *Carbon*, 2010, **48**, 4466–4474.
- 31 C. Liu, F. Hao, X. Zhao, Q. Zhao, S. Luo and H. Lin, *Sci. Rep.*, 2014, **4**, 3965.
- 32 Y. Chen, X. Zhang, D. Zhang, P. Yu and Y. Ma, *Carbon* 2010, **49**, 573–580.
- 33 J. Gao, F. Liu, Y. Liu, N. Ma, Z. Wang and X. Zhang, *Chem. Mater.*, 2010, **22**, 2213–2218.
- 34 J. Zhang, H. Yang, G. Shen, P. Cheng, J. Zhang and S. Guo *Chem. Commun.*, 2010, **46**, 1112–1114.
- 35 A. Esfandiari, O. Akhavan and A. Irajizad, *J. Mater. Chem.*, 2011, **21**, 10907–10914.
- 36 O. Akhavan, E. Ghaderi, S. Aghayee, Y. Fereydooni and A. Talebi, *J. Mater. Chem.*, 2012, **22**, 13773–13781.
- 37 M. F. Abdullah, R. Zakaria and S. H. S. Zein, *RSC Adv.*, 2014, **4**, 34510–34518.
- 38 O. Akhavan, E. Ghaderi, E. Abouei, S. Hatamie and E. Ghasemi, *Carbon*, 2014, **66**, 395–406.
- 39 J. Liu, S. Fu, B. Yuan, Y. Li and Z. Deng, *J. Am. Chem. Soc.*, 2010, **132**, 7279–7281.
- 40 M. A. Tabrizi and Z. Zand, *Electroanalysis*, 2014, **26**, 171–177.
- 41 E. C. Salas, Z. Sun, A. Lüttge and J. M. Tour, *ACS Nano*, 2010, **4**, 4852–4856.
- 42 C. K. Chua and M. Pumera, *J. Mater. Chem.*, 2012, **22**, 23227–23231.
- 43 P. Cui, J. Lee, E. Hwang and H. Lee, *Chem. Commun.*, 2011, **47**, 12370–12372.
- 44 I. K. Moon, J. Lee, R. S. Ruoff and H. Lee, *Nat. Commun.*, 2010, **1**, 73.
- 45 G. Zhao, D. Shao, C. Chen and X. Wang, *Appl. Phys. Lett.*, 2011, **98**, 183114.
- 46 Q. Qng, X. Wang, Z. Chai and W. Hu, *Chem. Soc. Rev.*, 2013, **42**, 8821–8834.
- 47 S. Yang, C. Zhu, J. Sun, P. He, N. Yuan, J. Ding, G. Ding and X. Xie, *RSC Advances*, 2015, **5**, 33347–33350.
- 48 R. Appel, *Angew. Chem. Int. Ed.*, 1975, **14**, 801–811.
- 49 J. M. Aizpurua and C. Palomo, *Synthetic*, 1982, 684–687.
- 50 E. S. Philip and E. O. James, *J. Org. Chem.*, 1976, **41**, 3279–3283.
- 51 G. A. Wiley, R. L. Hershkowitz, B. M. Rein and B. C. Chung, *J. Am. Chem. Soc.*, 1964, **86**, 964–965.
- 52 W. S. Hummers and R. E. Offeman, *J. Am. Chem. Soc.*, 1958, **80**, 1339–1339.
- 53 S. Leila and A. A. Anjali, *Int. J. Renew. Energy Environ. Eng.* 2014, **2**, 58–63.
- 54 E. Gotschi, C. Jenny, P. Reindl and F. Ricklin, *Helv. Chim. Acta.*, 1996, **79**, 2219–2234.
- 55 J. G. Henkel, J. T. Hane and G. Gianutsos, *J. Med. Chem.*, 1982, **25**, 51–56.
- 56 X. Hu, Z. Jiang, Z. Jia, S. Huang, X. Yang, Y. Li, L. Gan, S. Zhang and D. Zhu, *Chem. Eur. J.*, 2007, **13**, 1129–1141.
- 57 R. D. Parto and A. J. Speziale, *J. Am. Chem. Soc.*, 1965, **87**, 5068–5075.
- 58 S. P. Dhuru, K. J. Padiya and M. M. Salunkhe, *J. Chem. Res.*, 1998, 56.
- 59 R. D. Khachicyan, N. V. Tovmasyan and M. G. Indzhikyan, *Russ. J. Gen. Chem.*, 2007, **77**, 1034–1036.
- 60 F. Liu and T. Seok, *Adv. Funct. Mater.* 2010, **20**, 1930–1936.
- 61 G. I. Titelman, V. Gelman, S. Bron, R. L. Khalfin, Y. Cohen and H. Bianco-Peled, *Carbon*, 2005, **43**, 641–649.
- 62 E. Fuente, J. A. Menendez, M. A. Diez, D. Suarez and M. A. Montes-Moran, *J. Phys. Chem. B*, 2003, **107**, 6350–6359.
- 63 T. Szabo, O. Berkesi and I. Dekany, *Carbon*, 2005, **43**, 3186–3189.